Yogita Kalra

final thesis (VX)

PHD

Document Details

Submission ID
trn:oid:::27535:140617910

Submission Date
May 27, 2026, 11:23 AM GMT+5:30

Download Date
May 27, 2026, 11:25 AM GMT+5:30

File Name
final thesis (VX).pdf

File Size
2.0 MB

32 Pages

7,394 Words

41,954 Characters

7% Overall Similarity

The combined total of all matches, including overlapping sources, for each database.

Filtered from the Report

- Bibliography
- Small Matches (less than 9 words)

Match Groups

31 Not Cited or Quoted 6%
Matches with neither in-text citation nor quotation marks

8 Missing Quotations 1%
Matches that are still very similar to source material

0 Missing Citation 0%
Matches that have quotation marks, but no in-text citation

0 Cited and Quoted 0%
Matches with in-text citation present, but no quotation marks

Top Sources

3% Internet sources
6% Publications
3% Submitted works (Student Papers)

Integrity Flags

0 Integrity Flags for Review

Our system's algorithms look deeply at a document for any inconsistencies that would set it apart from a normal submission. If we notice something strange, we flag it for you to review.

A Flag is not necessarily an indicator of a problem. However, we'd recommend you focus your attention there for further review.

Match Groups

- **31** Not Cited or Quoted 6%
  Matches with neither in-text citation nor quotation marks
- **8** Missing Quotations 1%
  Matches that are still very similar to source material
- **0** Missing Citation 0%
  Matches that have quotation marks, but no in-text citation
- **0** Cited and Quoted 0%
  Matches with in-text citation present, but no quotation marks

Top Sources

3% Internet sources
6% Publications
3% Submitted works (Student Papers)

Top Sources

The sources with the highest number of matches within the submission. Overlapping sources will not be displayed.

1	Publication	Xin Guan, Suxia Xie, Junwu Zhuo, Siyi Sun. "Tunable circular dichroism supported ... 1%
2	Internet	www.mdpi.com <1%
3	Publication	Vishakha Sharma, Yogita Kalra, Ravindra Kumar Sinha. "Chiral perovskite based ... <1%
4	Publication	Youwen An, Wei Zhang, Tianjiao Du, Mingxuan Liu et al. "Soft-MEMS Chiral Reconf... <1%
5	Publication	Li, Yangcheng, Oleksiy Svitelskiy, David Carnegie, Edik Rafailov, Vasily N. Astratov... <1%
6	Internet	tesisenxarxa.net <1%
7	Student papers	Universitat Politècnica de València on 2021-02-08 <1%
8	Student papers	University of Greenwich on 2012-12-12 <1%
9	Internet	repositorio-iul.iscte.pt <1%
10	Internet	research.wsulibs.wsu.edu:8080 <1%

11	Student papers	City University of Hong Kong on 2022-07-19 <1%
12	Student papers	University of Glasgow on 2025-04-20 <1%
13	Student papers	University of Sheffield on 2025-04-17 <1%
14	Publication	Xiaoyong He, Wenhan Cao, Fangting Lin. "Tunable BIC metamaterials with Dirac s... <1%
15	Internet	www.researching.cn <1%
16	Publication	Katsuya Tanaka, Dennis Arslan, Stefan Fasold, Michael Steinert et al. "Chiral Bilay... <1%
17	Publication	Monyayi, Victor Tebogo. "Mathematical Analysis of Evolution Equations With Frac... <1%
18	Publication	Yu Geun Ki, Byeong Je Jeon, Il Hoon Song, Seong Jun Kim, Sangtae Jeon, Soo Jin Ki... <1%
19	Internet	link.springer.com <1%
20	Internet	proxy.osapublishing.org <1%
21	Publication	tian ma, Yizu Zou, Zihao Chen, IQRA Afzal, Doudou Wang, Depeng Kong, Li Ma, Ju... <1%
22	Publication	Christina Ioannou, Ranjith Nair, Ivan Fernandez-Corbaton, Mile Gu, Carsten Rock... <1%
23	Publication	Eylul Simsek, Keyong Zhu, Glareh N. Kashanchi, Megan J. Williams et al. "Light Tra... <1%
24	Publication	Isabelle Staude, Andrey E. Miroshnichenko, Manuel Decker, Nche T. Fofang et al. ... <1%

25 Student papers

Khalifa University of Science Technology and Research on 2025-11-24 <1%

26 Publication

Mikhail Y. Shalaginov, Sawyer D. Campbell, Sensong An, Yifei Zhang et al. "Design... <1%

27 Publication

Munseong Bae, Chia-Chun Pan, Chanik Kang, Jinseong Bae et al. "Inverse design f... <1%

28 Publication

Shiyu Yang, Jin Lv, Honghao Zhou, Jinlin Wang, Hao Wang, Yandong Zhang, Ning ... <1%

29 Student papers

University College London on 2016-09-04 <1%

30 Publication

Xiang Ni, Simon Yves, Alex Krasnok, Andrea Alù. "Topological Metamaterials", Ch... <1%

31 Internet

m.researching.cn <1%

ABSTRACT

Chiral metasurfaces enable compact manipulation of circularly polarized light; however, most designs rely on rigid platforms that limit their adaptability. Here, a mechanically reconfigurable single layer dielectric chiral metasurface based on polydimethylsiloxane (PDMS), operating in the near infrared region is proposed. The unit cell, comprising two angularly oriented hollow rectangular cavities, introduces symmetry breaking that enables strong chiroptical response. Numerical simulations show dual band circular dichroism (CD), with peak values of ~0.89 at 911 nm and −0.8 at 952 nm under oblique incidence. The metasurface exhibits high quality resonances with Q factors of 1495 and 4678, which remain largely preserved under mechanical stretching. Electric field analysis reveals distinct chiral resonant modes with opposite handedness preference, while parametric studies confirm the robustness of the dual band response against geometric variations. Owing to the intrinsic flexibility of PDMS, uniaxial deformation enables controlled spectral tuning of the CD response while maintaining strong polarization selectivity. The proposed design provides a simple and effective platform for flexible and tunable chiral photonic devices.

Keywords: Chiral metasurface, Circular dichroism, Jones matrix, Polarization control, Tunability, Q factor**.**

CHAPTER 1

INTRODUCTION

This chapter establishes the scientific and technological context for the research presented in this thesis. It begins with a broad background on metasurfaces and chiral optics, narrows to a precise problem statement, articulates the motivation for pursuing a flexible dielectric architecture, and presents an analytical review of the relevant literature that identifies the gap this work addresses. The chapter concludes with a statement of objectives, a delineation of the scope, and an outline of the thesis structure.

1.1 Background

One of the defining challenges in the field of modern photonics is to control light at nanoscale. Almost all of the conventional optical devices such as lenses, wave plates, beam splitters and polarizers depend on macroscopic material thickness to accumulate the phase retardation or polarization rotation to perform a specific function. These volume-based systems impose practical constraints on the miniaturization, integration, and multifunctionality of optical systems. Metasurfaces, conceived as two-dimensional arrays of subwavelength scale resonators (meta atoms) patterned on a planar substrate, offer an alternative route in which the relevant optical transformation is engineered at the interface itself rather than accumulated over propagation distance [1]– [4].

An incident wave can be given a precise phase, amplitude, or polarization with the help of a meta atom. On arranging these meta atoms in a periodic array, the surface can reproduce and often exceed the functionality of bulk optical elements despite being much compact and thinner than the

operating wavelength. This makes them capable of having multiple functionalities such as flat lenses with diffraction limited focusing [3], holographic beam shapers, quarter and half wave retarders, absorbers, nonlinear optical elements, and polarization converters. Cui et al. [2] extended this further by introducing programmable metasurfaces where a single reconfigurable surface could realise multiple electromagnetic functions when digitally encoded with phase distributions. Such developments show the potential of metasurfaces for next generation compact and adaptive photonic systems.

Out of all the types of metasurfaces, chiral metasurfaces hold a unique importance due to their innate nature to distinguish and manipulate circularly polarized electromagnetic waves. Chirality is the geometric property of an object that cannot be superimposed on its mirror image. This gives rise to two different interactions with left circularly polarized (LCP) and right circularly polarized (RCP) electromagnetic waves. In naturally occurring chiral materials such as sugars, amino acids, and DNA, these optical effects remain weaker at optical frequencies because the molecular dimensions are very much smaller in magnitude as compared to the wavelength of light. Chiral metasurface overcome this limitation as they can be engineered and amplify chiroptical responses by orders of magnitude within subwavelength thicknesses. This enables them to be used in applications ranging from compact circular dichroism spectroscopy and chiral molecular sensing to optical information encoding and quantum optical state preparation [11]– [14].

Increasing attention has been directed towards the development of photonic systems that are capable of operating on non-planar and dynamically deformable surfaces along with the need for stronger chiroptical responses. The demand for optical functionality on substrates that bend, stretch, and deform during operation is increasing in applications such as wearable health monitors, smart contact lenses, flexible displays, and bio integrated optical sensors. Polydimethylsiloxane (PDMS)

has established itself as the elastomeric substrate of choice for such applications: it is optically transparent across the visible and near infrared spectrum, chemically inert, biocompatible, and capable of sustaining strains exceeding 100% without mechanical failure [29], [30]. When subwavelength features are patterned directly into PDMS—rather than deposited as thin film resonators on its surface—the result is a purely dielectric flexible metasurface in which the resonator and the substrate are the same material, eliminating delamination failure modes and ohmic losses simultaneously.

1.2 Problem Statement

Despite rapid progress in both chiral metasurface research and flexible photonics, a persistent gap exists at their intersection. Most chiral metasurfaces reported to date are built on rigid, non-deformable substrates like silicon, glass, or quartz or consist of metallic resonators which result in ohmic losses. Designs that utilise flexible substrates have a hybrid structure consisting of metallic or high index semiconductor resonators fabricated separately and then transferred or deposited onto PDMS or other elastomers [26]– [29]. Such hybrid configurations retain the disadvantages of their metallic components. Another shortcoming of existing flexible chiral metasurfaces is that nearly all reported designs exhibit a single band CD response. Dual band circular dichroism that is two spectrally separated peaks with opposite CD signs is desired for differential sensing and multi-channel filtering but has been achieved almost exclusively in multilayer stacked geometries whose fabrication is complicate. Realizing strong dual band CD in a single layer, dielectric, elastomeric structure constitutes a challenge that this thesis directly addresses.

1.3 Motivation

The motivation for this work is grounded in two converging practical demands. First, there is a need for tunable circular dichroism elements that can be integrated into compact and mechanically compatible photonic devices. Emerging applications in wearable circular dichroism spectroscopy for continuous health monitoring, in flexible polarimetric imagers for defence and autonomous vehicles, and in conformable optical coatings for augmented reality systems all require polarization selective optical elements that combine large CD contrast with mechanical adaptability, a combination that existing technology does not provide.

Second, the near infrared region between 900 nm and 1100 nm is of exceptional technological importance. It overlaps with the first and second biological transparency windows relevant to tissue penetrating optical biosensors, with the operating wavelengths of silicon photonic integrated circuits, and with the short wave infrared bands used in machine vision and LiDAR. Achieving strong dual band CD in this spectral range using a purely dielectric, single layer flexible structure without recourse to high index crystalline semiconductors such as silicon or titanium dioxide, which are mechanically incompatible with large deformation elastomeric processing is both scientifically nontrivial and practically consequential. The PDMS based platform examined in this study offers a realistic path to implement such devices, particularly through soft lithography or nanoimprint techniques compatible with manufacturing.

1.4 Literature Review

1.4.1 Metasurfaces: Foundations and Programmability

Metasurfaces were developed as a counterpart to metamaterials which also showed that their periodic arrangements of subwavelength resonators could produce unnatural properties like negative refractive indices, zero permittivity, etc. The evolution of metamaterials from microwave to visible

frequency regimes was given by Soukoulis and Wegener [5] who gave comprehensive analysis while also identifying the fabrication challenges in 3d architectures. Their analysis suggested the growing transition towards two dimensional metasurface which preserve the resonant behaviour of metamaterials while reducing fabrication complexities.

The programmable and coding metasurface concept articulated by Cui et al. [2] marked a conceptual inflection point. By representing the phase response of meta atoms in a single or multi level digital framework, they showed that a single reconfigurable surface could perform beam steering, holography, and programmable diffraction through a change of the coding pattern rather than a change of the physical structure. Basar et al. [1] subsequently extended this vision to the domain of wireless communications, proposing that reconfigurable intelligent surfaces could reshape electromagnetic propagation channels in real time. Sharma et al. [3] showd the design of a human eye inspired concentric cylindrical metalens, while Ai et al. [4] reviewed the application of metasurfaces in future display technologies, collectively illustrating the application of metasurface engineering in a vast space.

1.4.2 Dielectric Metasurfaces and the Transition Beyond Plasmonics

The limitations of plasmonic designs at optical and near infrared frequencies, principally the ohmic losses that suppress transmission efficiency and broaden resonance linewidths have driven extensive interest in all dielectric metasurfaces. Zheludev [6] argued that overcoming material loss constraints is a challenge for the advancement of the metamaterial and metasurface. The breakthrough came with the study by Kuznetsov et al. [8], that high refractive index dielectric nanoparticles support spectrally overlapping electric and magnetic dipole Mie resonances that can

24

be engineered to produce constructive or destructive interference in forward and backward scattering directions without the ohmic penalties of metals.

This Mie resonance framework has since been generalized to a wide range of dielectric geometries and materials. Xing et al. [7] further demonstrated highly reflective all dielectric metasurfaces based on diamond resonators in the near infrared, showing that the Mie approach extends to wide bandgap materials whose transparency windows are relevant for specific spectral applications and not restricted to silicon only.

1.4.3 Chiral Metasurfaces and Circular Dichroism

Metasurfaces have evolved into a field in itself because of the numerous ongoing studies taking place ranging from plasmonic, dielectric and hybrid material systems. Nanostructured chiral materials were studied by Petronijevic et al. [12] ranging from individual nanoparticles to extended arrays which clarified the geometric conditions required to achieve strong cd and a distinction was made between intrinsic chirality which arises from three-dimensional asymmetry of individual meta atoms, and extrinsic chirality, which arises from oblique incidence. Kong et al. [13] studied chirality in plasmonic systems assembled through biological templates and abiotic fabrication and showed that CD responses are significantly greater than those produced by individual particles because of the electromagnetic coupling between resonators within a chiral configuration. Zhu et al. [14] also observed that a purely planar dielectric nanostructure under oblique illumination could produce giant intrinsic chiroptical activity.

Gorkunov et al. [11] showed that quasi bound states in the continuum (quasi BIC) in dielectric metasurfaces can support near lossless maximum chirality. Light can effectively be trapped using BIC structures. They allow controlled coupling to external light by slightly breaking

symmetry while maintaining extremely high Q resonances with lower losses compared to plasmonic structures. This insight explains why purely dielectric chiral metasurface can, in principle, achieve the same or larger CD magnitudes as their plasmonic counterparts while operating with far lower losses.

Within the research group of the present authors, Sharma [15] investigated chiral perovskite based metasurface exhibiting simultaneous linear and circular dichroism. The structure was designed by controlling symmetry and symmetry breaking to obtain chirality. Recent reviews by Hu et al. [16] and Deng et al. [17] have fully outlined the state of the art in dielectric chiral metasurfaces, with Hu et al. emphasising single layer configurations as an emerging research priority, and Deng et al. drawing an important distinction between broadband polarization conversion and resonant high Q CD designs, concluding that the latter offers superior performance for sensing applications. Tonkaev et al. [18] pushed the frontier further into nonlinear regimes, fabricating chiral metasurfaces from van der Waals materials to show chirality selective nonlinear harmonic generation.

1.4.4 Active and Tunable Metasurfaces

Most metasurface have a static optical which constitutes a fundamental limitation for adaptive photonic applications. Hail et al. [9] and Kang et al. [10] provided complementary surveys of active optical metasurfaces, documenting tuning mechanisms that include phase change material switching, electro optic modulation, thermo optic effects, micro electromechanical actuation, and optical pumping. Badloe et al. [19] gave a roadmap for fully active nanophotonics, identifying mechanical deformation as particularly attractive for near infrared applications because it can produce large, continuous, and reversible spectral shifts through simple strain control. Practical implementations of active metamaterials were surveyed by Fadhil and Al Sahlawi [20], while

Kowerdziej et al. [21] showed that electrically switchable phase and amplitude responses can be produced with soft matter over layers like liquid crystals, when integrated with metasurface.

Li et al. [23] reviewed active tunable metamaterials based on graphene, phase change materials, and semiconductors, and He et al. [24] showed tunable BIC metamaterials incorporating Dirac semimetals as the active medium for terahertz frequencies. Fan et al. [25] argued that the transition from static to dynamically reconfigurable metasurfaces is the defining challenge for the next generation of flat optical devices. Qin et al. [22] introduced the intriguing concept of microfluidic metasurfaces in which on chip fluid flow reconfigures the electromagnetic response in real time, though the integration complexity of fluidic channels within a compact photonic platform remains a practical obstacle.

1.4.5 Mechanically Flexible and Stretchable Chiral Metasurfaces

The intersection of mechanical flexibility and chiroptical response has been explored in a growing number of studies, predominantly at terahertz and mid infrared frequencies where fabrication tolerances are more relaxed. Han et al. [26] showed that mechanical deformation of propeller shaped terahertz metamaterials patterned on flexible substrates can induce and tune circular dichroism because the deformation itself breaks the structural symmetry of an otherwise achiral design. This deformation induced chirality mechanism is conceptually distinct from the intrinsic symmetry breaking strategy employed in the present work, where the meta atom is chirally designed from the outset and deformation is used as a spectral tuning tool.

Li et al. [27] reported a mechanically reconfigurable chiral metasurface exhibiting large range switchable CD, showing on/off switching of the chiroptical response through structural reconfiguration. However, their design utilised metallic resonators on a flexible substrate, inheriting

the ohmic losses of the metallic components. Liu et al. [28] achieved Fano enhanced CD in deformable stereo metasurfaces, exploiting the spectral asymmetry of Fano resonances to achieve exceptionally sharp CD line shapes during mechanical deformation—again in a metallic architecture.

Guan et al. [29] investigated a stretchable PDMS based metasurface supporting quasi BIC modes with tunable CD. Their study showed that a purely dielectric PDMS structure can be used for mechanically tuning the optical response of the metasurface as mechanical stretching produced controlled spectral shifts of the CD peak in a purely dielectric PDMS structure. However, the CD values reported were for a single band only.

1.4.6 PDMS as a Photonic Platform

PDMS has been well characterized as an optical material for fabrication of photonic device. The complex refractive indices of a variety of polymers including PDMS were measured by Zhang et al. [30] measured in the visible and near infrared spectral bands. The results confirmed that PDMS is mostly lossless in the NIR region of interest. The material dispersion data has been used directly in the present simulations. The ratio of base to curing 10:1 agent used here results in a Young's modulus in the range of approximately 1–2 MPa which provides strain tuning while maintaining the structural uniformity of the nanoscale cavity geometries over multiple deformations.

Xu et al. [34] gave a quantitative mechanical framework for stretchable PDMS based metamaterials, showing a linear relationship between applied stress and strain and providing the constitutive equation that relates the geometric reconfiguration of the meta atom to the applied strain. Plum et al. [31] studied the optical response in achiral metasurfaces where it demonstrated how the illumination affects the response at oblique incidence in activating or it. Jones calculus was

developed by Menzel et al. [32] specifically for periodic metamaterial layers establishing the theoretical formalism used in the present work to extract circular dichroism from linear polarization transmission coefficients. Ardakani and Moradi [33] showed strong CD in a non-chiral metasurface exploiting metallic V shaped nanostructures, providing an instructive contrast case that highlights the different physical origins of extrinsic versus intrinsic chirality.

1.5 Research Gap

The foregoing review reveals four specific gaps that motivate the present investigation. First, while PDMS based flexible metasurfaces have been studied in the context of tunable CD [29], the designs reported to date achieve high CD magnitudes and exhibit single band responses. Achieving near unity dual band CD in a purely dielectric PDMS single layer configuration has not been showed. Second, mechanically tunable chiral metasurfaces that operate in the near infrared range (900–1100 nm) without any metallic inclusions are essentially absent from the literature, a gap that is significant given the technological importance for biosensing and silicon photonics.

Third, the differential sensitivity of co-existing chiral modes in a single layer metasurface to uniaxial stretching along orthogonal axes i.e., the anisotropy of the chiroptical mechanical coupling has not been systematically analysed. This anisotropy is potentially exploitable for vector strain sensing, but the structural geometrical factors that govern it are not understood. Fourth, the quality factor evolution of chiral resonances in a flexible dielectric metasurface under strain, a parameter of central importance for spectral resolution in sensing applications, has not been reported. The present thesis addresses all four gaps through the design and numerical analysis of a PDMS based single layer chiral metasurface in the NIR.

1.6 Objectives

The specific objectives of this research are as follows:

(1) To design a single layer PDMS based chiral metasurface unit cell that simultaneously breaks in plane and out of plane symmetries through an asymmetric hollow cavity geometry and achieves strong dual band circular dichroism in the NIR range of 900–1100 nm.

(2) To develop and apply the Jones matrix analytical framework for extracting and interpreting the circular polarization transmission properties of the proposed metasurface from full wave numerical simulations.

(3) To perform a systematic parametric investigation of the cavity dimensions governing each chiral mode, characterizing the sensitivity of the CD spectrum to geometric variations and deriving design guidelines for spectral positioning and amplitude control.

(4) To simulate the chiral response under uniaxial stretching along the x and y axes, analysing the resultant spectral shifts, CD amplitude changes, and quality factor progression of both modes.

1.7 Scope of Work

This thesis proposes the numerical design and theoretical analysis of a PDMS-based chiral metasurface. Experimental fabrication and characterization are beyond the present scope, though the selected geometric parameters are consistent with features achievable by direct laser writing, electron beam lithography, or nanoimprint lithography in PDMS. Electromagnetic simulations were performed using CST Microwave Studio which uses finite element method to solve. The spectral analysis was done in the NIR range of 900–1100 nm. Mechanical stretching has been modelled through geometric scaling of unit cell dimensions according strain definition and explicit finite

element mechanical simulations are not performed. Only uniaxial stretching conditions (along x and y separately) are considered.

1.8 Organisation of the Thesis

The structure of the thesis is as follows. The proposed metasurface design including the geometry of the unit cell, the theoretical framework for polarization analysis and the simulation methodology has been presented in Chapter 2. Numerical results, the parametric sensitivity study, the mechanical tunability characterization and Q factor analysis are shown in Chapter 3. The summary of the entire work has been provided in chapter 4 which also gives a direction for implementation of the work. A complete list of references is provided at the end of the document.

The present chapter establishes the scientific context and precise motivation for the work, reviewed the state of the art to identify the research gap, and stated the objectives and scope of the thesis. The subsequent chapters build systematically upon this foundation.

CHAPTER 2

PROPOSED WORK: DESIGN, METHODOLOGY, AND RESULTS

This chapter presents the main research contribution of the thesis. It describes the material and the geometry of the metasurface, followed by theoretical framework and computation of transmission characteristics. It describes the formulation of Jones matrix which is used to describe the transmission characteristics of a metasurface in linear basis which can be converted into circular basis by unitary transformation. The matrix then gives us complex fields from which circular dichroism can be calculated. Further, a simplified stretching behaviour is described to analyse the tunability of the metasurface.

2.1 Material Platform: Polydimethylsiloxane

The material used here is PDMS (polydimethylsiloxane) having a base to cure agent ration of 10:1 [30]. The measurement of refractive index carried out by Zhang et al. [30] have been used directly in the simulation to represent the material correctly.

It is possible to use a single material instead of a metallic resonator or nanorods embedded or deposited on a dielectric substrate. It eliminates ohmic losses, reduces the fabrication process to a single soft lithographic or nanoimprint patterning step, and ensures that the resonator deforms identically with the substrate under mechanical strain, avoiding the stress concentrations and delamination failure modes that arise in metal on elastomer hybrid systems.

2.2 Unit Cell Geometry and Symmetry Analysis

The unit cell geometry is shown in Figure 1. Each meta atom has a cuboidal geometry with periodicity $p_x = p_y = p = 800\ nm$; the structure height is $h = 500\ nm$. The top surface of the cuboid has two hollow rectangular cavities are engraved to prescribed depths into the PDMS bulk. The use of hollow cavities instead of nanopillars inverts the conventional metasurface geometry: the cavities define regions of reduced effective refractive index responsible for governing the resonant mode of the structure while the dielectric PDMS forms the host structure.

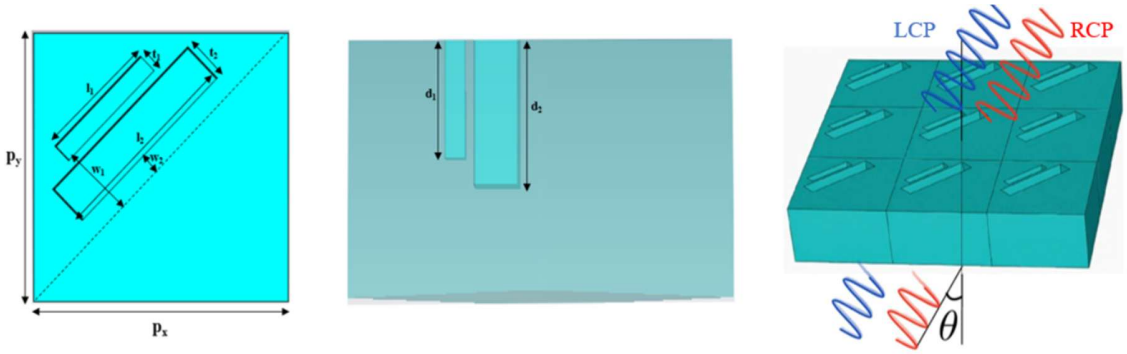

Figure 1. (a) top view of the proposed unit cell, (b) side view of the unit cell showing depth of cavities, (c) Schematic of the proposed PDMS based chiral metasurface subjected to LCP and RCP.

The dimensions of the upper cavity are $l_1 \times t_1 \times d_1 = 190\ nm \times 60\ nm \times 230\ nm$ where l_1, t_1 and d_1 are the length, width and depth of the upper cavity. The lower cavity has *dimensions* $l_2 \times t_2 \times d_2 = 300\ nm \times 130\ nm \times 285\ nm$. Both cavities are oriented at 45° to the principal in plane axes of the unit cell. The combination of lateral translation and vertical separation introduces chirality in the structure: the upper cavity is first translated by $y_1 = 20\ nm$ along the y axis before rotation, while the lower cavity is translated by $y_2 = 20\ nm$ along y before its own rotation. This configuration breaks three distinct symmetries: (i) the in-plane mirror symmetry along x, because the two cavities are translated by different lengths along y direction; (ii) the in-plane mirror symmetry along y, because the rotated cavities are not symmetric about the y axis; and (iii) the rotational symmetry about the vertical axis, because the two cavities have different depths. The simultaneous breaking of in plane

and out of plane symmetries is the necessary and sufficient condition for a planar structure to exhibit strong intrinsic chirality under oblique illumination [31]. The chirality of the structure cannot be removed by any in plane translation or rotation which differentiates this design from extrinsically chiral configurations where the CD arises because of oblique incidence.

2.3 Theoretical Framework

2.3.1 Jones Matrix Formalism

The transmission properties of the metasurface are analysed using the Jones matrix formalism following Menzel et al. [32]. When a metasurface is illuminated by a monochromatic plane wave, the relationship between the complex amplitudes of the transmitted and incident electric fields in the orthogonal linear polarization basis $\{\hat{x}, \hat{y}\}$ is described by the 2×2 Jones transmission matrix:

$$T = \begin{pmatrix} t_{xx} & t_{xy} \\ t_{yx} & t_{yy} \end{pmatrix} \quad (1)$$

where t_{ij} $(i, j \in \{x, y\})$ denotes the complex transmission coefficient for light incident with j polarization and transmitted with i polarization. Direct transmission without polarization conversion are described by co polarized coefficients t_{xx} and t_{yy}, while the conversion between orthogonal states is given by cross polarized coefficients, t_{xy} and t_{yx}.

To evaluate the response under circularly polarized illumination, the linear basis transmission matrix is transformed into the circular polarization basis using the standard unitary transformation. The resulting circular Jones matrix is [32]:

$$J_{circ} = \begin{pmatrix} t_{RR} & t_{RL} \\ t_{LR} & t_{LL} \end{pmatrix} = \frac{1}{2}\begin{pmatrix} (t_{xx} + t_{yy}) + i(t_{xy} - t_{yx}) & (t_{xx} - t_{yy}) - i(t_{xy} + t_{yx}) \\ (t_{xx} - t_{yy}) + i(t_{xy} + t_{yx}) & (t_{xx} + t_{yy}) - i(t_{xy} - t_{yx}) \end{pmatrix} \quad (2)$$

The diagonal elements t_{RR} and t_{LL} represent co circular (handedness preserving) transmission, while the off-diagonal elements t_{RL} and t_{LR} capture circular polarization conversion. The total transmittances for RCP and LCP incident light, summing contributions from both output polarization channels, are given by:

$$T_R = |t_{RR}|^2 + |t_{LR}|^2 \quad (3)$$

$$T_L = |t_{LL}|^2 + |t_{RL}|^2 \quad (4)$$

2.3.2 Circular Dichroism Definition and Quality Factor

Circular dichroism, quantifying the handedness selectivity of the metasurface response, is defined as the differential transmittance [33]:

$$CD = T_R - T_L \quad (5)$$

A positive CD value implies that RCP light is transmitted while RCP light is suppressed whereas negative CD implies preferential transmission of LCP while RCP is suppressed. If a structure is symmetric, both LCP and RCP light interact with the system in the same way. They excite degenerate resonant modes having the same frequency. As a result, there is no difference in how the system responds to left and right polarization and the CD is 0 across the entire spectrum. The deliberate breaking of symmetry in the structure makes it as asymmetric because of which it does not treat both polarizations equally and produces spectrally distinct resonant responses for the two handedness states and gives non-zero CD at each resonant frequency. The quality factor of each

resonance mode is defined as $Q = \lambda_0/\Delta\lambda$, where λ_0 is the resonant wavelength and $\Delta\lambda$ is the corresponding full width at half maximum.

2.3.3 Mechanical Strain Model

The relation between applied stress δ_i, strain ε_i along direction i ϵ {x, y} and the Young's modulus E is defined as $\varepsilon_i = \delta_i/E$ [34]. Since PDMS is nearly incompressible (Poisson's ratio $\nu \approx 0.5$), strain in one direction induces equal and opposite strain in the transverse in plane direction. Numerical modelling of the system can be done by scaling the unit cell dimensions along x and y directions and the optical response of the modified geometry is recalculated. For mathematical simplification, the stretching strain has been defined as the ratio of the change in length after stretching to the initial length of the structure [34]:

$$\varepsilon = \frac{l - l_0}{l_0} \tag{7}$$

where l_0 is the initial length and l is the post deformation length along the stretching direction.

2.4 Simulation Setup

All electromagnetic simulations were performed in CST Microwave Studio using the frequency domain solver. Periodic boundary conditions were applied along x and y axis to represent infinite periodic array in the horizontal plain while open boundary condition was applied along the z axis. The structure was excited by a plane wave propagating along the z axis and incident at an angle of 55° to the z axis, which was identified through an angular parametric sweep as the angle that maximises the CD for the present geometry. This is consistent because oblique incidence is responsible for breaking external symmetry and improving chiroptical response [31]. The wavelength sweep covered 900 1100 nm.

CHATPER 3

3.1 Results and Analysis

3.1.1 Transmission Coefficients and Dual Band CD Response

To understand the response of the metasurface, particularly its circular dichroism (CD) response, transmission of LCP and RCP light was analysed. Figure 2 (a) shows the transmission coefficients obtained under circular polarized illumination, which were obtained by converting the linear polarization Jones matrix components (t_{xx}, t_{xy}, t_{yx}, t_{yy}) into circular polarization basis. Figure 2 (b) shows the transmission plot of LCP and RCP light, which is obtained with the help of equations 2 and 3. At the shorter wavelength resonance, the right circularly polarized light is transmitted more than the left circularly polarized light. In contrast, at the longer wavelength resonance, the left circularly polarized light is transmitted more than the right circularly polarized light. This behaviour, namely the selective transmission of a polarization state, arises from distinct chiral modes with opposite handedness preferences. As a result, the observed dual band CD originates from polarization dependent interference between the resonant modes.

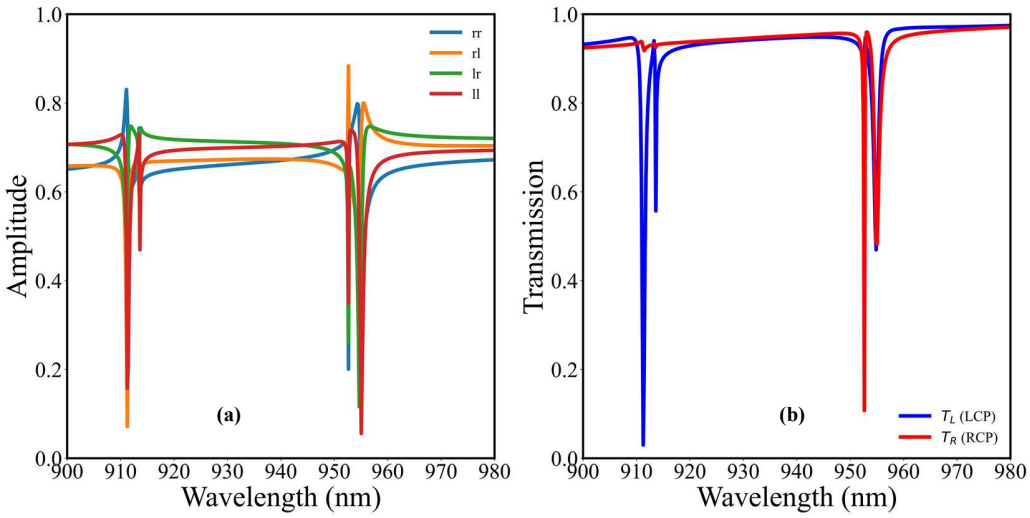

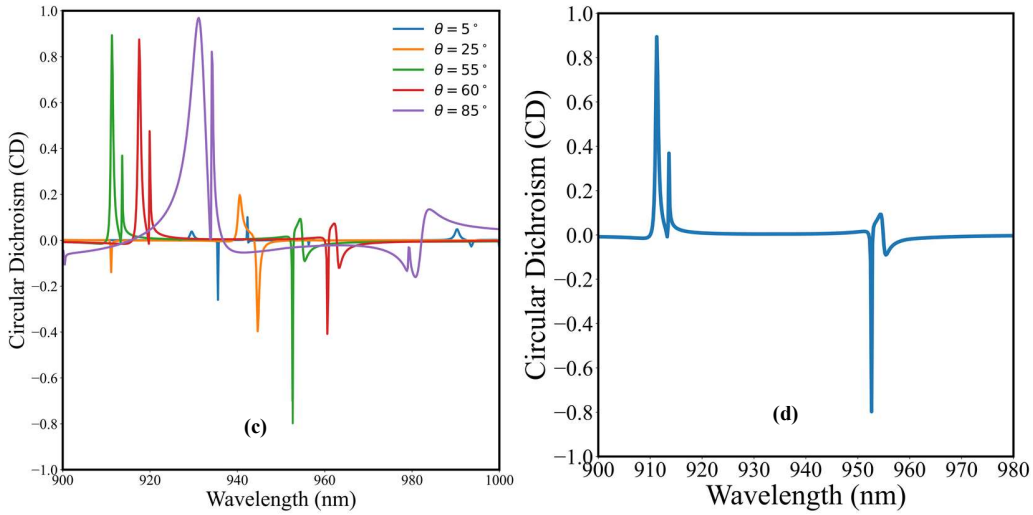

Figure 2. (a) plot of amplitude of transmission coefficients, (b) transmission of LCP and RCP light, (c) CD vs wavelength for different incident angles, (d) CD vs wavelength for optimized geometry.

Figure 2(c) proves how oblique incidence introduces chirality externally as resonance peaks shift and their amplitudes change significantly and shows that the optimized result obtained corresponds to 55^0. A maximum CD of +0.89 near 911 nm (mode 1) implies that RCP light transmits through the structure and a negative peak of CD of −0.8 near 953 nm (mode 2) implies LCP light transmits more. These values are notably high for a single layer, purely dielectric structure. The quality factors $Q_1 \approx 1495$ (mode 1) and $Q_2 \approx 4678$ (mode 2) indicate spectrally sharp resonances, with mode 2 being substantially more confined.

3.1.2 Electric Field Distributions

Figure 3 shows electric field distribution in the metasurface. The electric field confinement is relatively weaker under RCP compared to LCP which leads to stronger resonant scattering under LCP at 911 nm resulting in less transmission under LCP whereas the electric field confinement is relatively weaker under LCP compared to RCP at 953 nm which leads to less transmission under RCP.

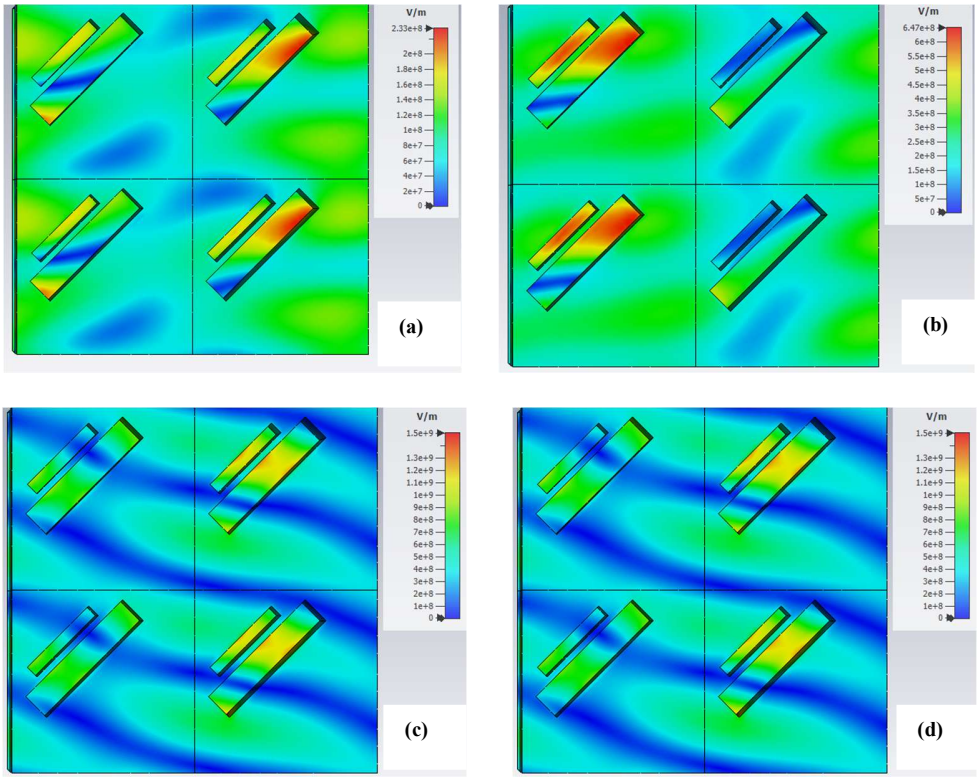

Figure 3. (a) Electric field distribution for the metasurface structure at 911 nm under RCP light. (b) Electric field distribution for the metasurface structure at 952 nm under LCP light.

3.2 Parametric Study

To investigate the behaviour of the structure's chiroptical response on geometry, a parametric study was performed by varying the geometry of upper and lower cavities while the other parameters were kept fixed.

3.2.1 Influence of Upper Cavity Dimensions

The variation of depth of upper cavity d_1 shows a gradual spectral shift of both mode 1 and mode 2 with increasing depth. This suggests that the chiral resonant modes responsible for such behaviour are resilient to changes in the upper cavity depth. Both modes shift towards longer wavelengths as d_1 rises, which implies a longer effective optical path and modified phase

accumulation within the cavity. It is to be noted that the magnitude of the CD bands is only slightly impacted, but the spectral positions are closely spaced.

The influence of the upper cavity length l_1 was also examined, showing a stable dual band response with gradual spectral shifts for both CD bands with small changes in the magnitude for mode 1 and moderate changes in mode 2.

The metasurface maintains its dual band CD response with small spectral shifts for t_1. Mode 1 remains nearly constant whereas the 2nd mode experiences modulation, indicating that variations in cavity thickness primarily affect, even though the geometric tuning modifies the confinement and leakage, the chirality mechanism remains the same.

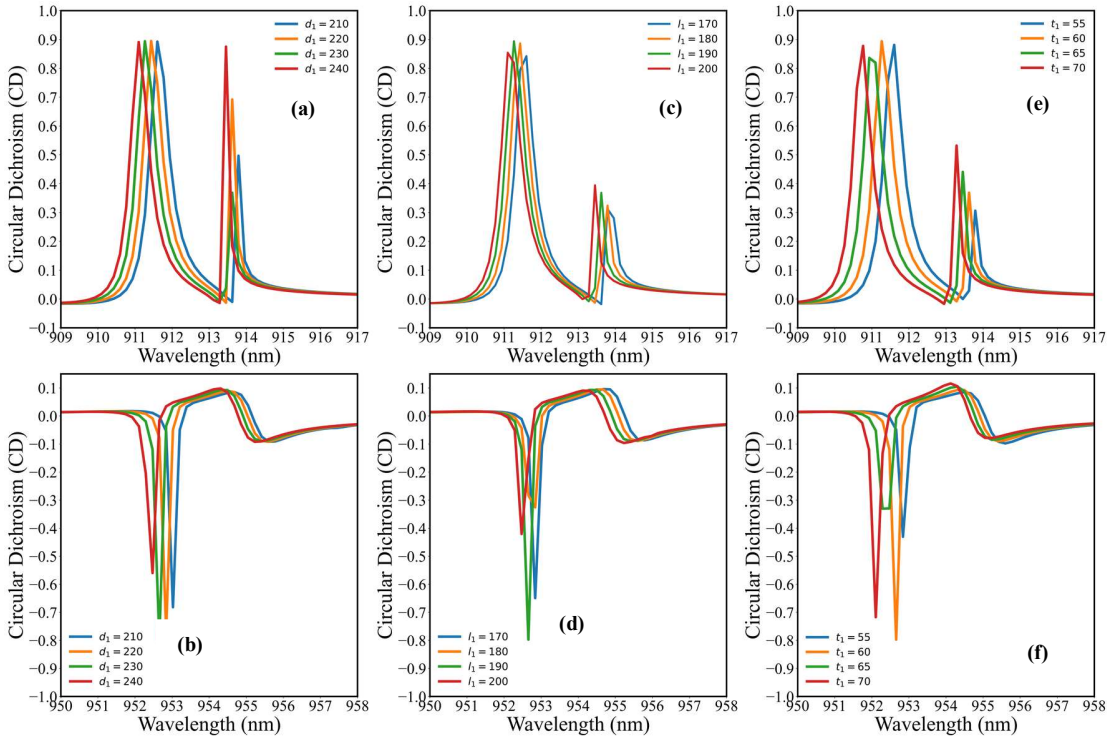

Figure 4. CD vs wavelength curve for variation of geometric parameters for upper cavity. (a), (c) and (e) show variation of positive band whereas (b), (d) and (f) show variation of negative band.

3.2.2 Influence of Lower Cavity Dimensions

On varying the depth of the lower cavity d_2, the metasurface retains a distinct dual band CD response, confirming the structural stability of the chiral resonances, like that observed in the variations in d_1. Contrary to the variations in the upper cavity depth, increasing d_2 causes more noticeable spectral modulation. At longer wavelength, the mode 2 shows increased sensitivity, as it experiences greater wavelength shifts and shows more pronounced changes in the magnitude of CD. This suggests that the corresponding chiral mode is more sensitive to the depth induced phase changes because it has stronger field confinement within the lower cavity region. Figure 5 presents the corresponding parametric study for lower cavity parameters (l_2, t_2, d_2). The response of mode 1 to lower cavity variations is again modest: spectral positions shift slightly but peak CD amplitudes are largely preserved. This reinforces the interpretation of mode 1 as a globally determined, topologically robust chiral mode whose coupling efficiency is insensitive to the dimensions of either individual cavity in isolation.

The impact of lower cavity length L2 on the CD response is much more noticeable as compared to changes in L1. The metasurface maintains the dual CD spectrum over the entire parameter range showing significant spectral shifts on increasing L2 for both CD bands, especially for the longer wavelength i.e. negative CD resonance. The circular dichroism magnitude remains high despite this enhanced tunability because the chiral modes are well defined, which shows that spectral control can be achieved without affecting the strength of the chiral response.

The metasurface maintains its dual band CD response with small spectral shifts for t_2. The positive CD bands remain nearly constant whereas the negative CD band experiences modulation, indicating that variations in cavity thickness primarily affect, even though the geometric tuning modifies the confinement and leakage, the chirality mechanism remains the same.

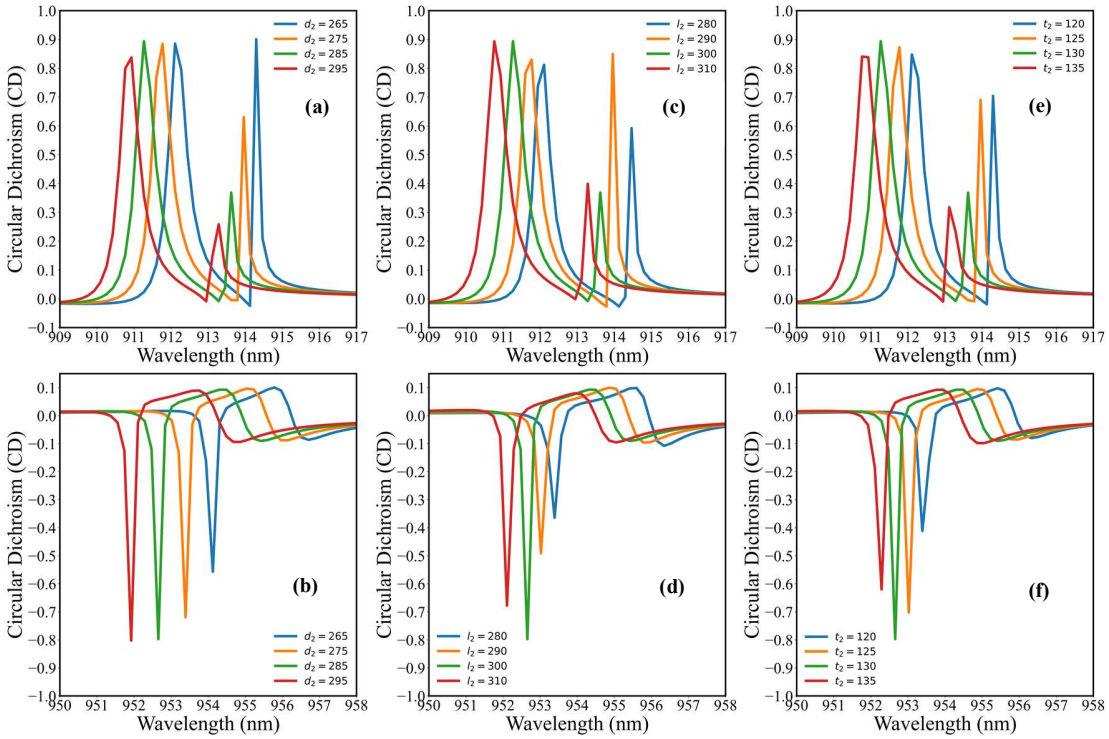

Figure 5. CD vs wavelength curve for variation of geometric parameters for the lower cavity. (a), (c) and (e) show variation of the positive band, whereas (b), (d), and (f) show variation of the negative band.

3.3 Mechanical Tunability

Since PDMS is flexible, its mechanical properties can be used to regulate the CD phenomenon through stretching using the relation given by (34):

$$\varepsilon_i = \frac{\delta_i}{E} \tag{6}$$

where $i \in x, y$, the Young's modulus is given by E, ε_i is the ratio of change in area to initial area and δ_i is the strain force of PDMS. When the structure is subjected to tensile stress along x axis, it stretches along the x direction while its y components remain fixed. The same is true when tensile stress is along y axis. For mathematical simplification, stretching strain has been defined as the ratio of the change in length after stretching to the initial length of the structure (29):

$$\varepsilon = \frac{l - l_0}{l_0} \tag{7}$$

where l is the final length of the structure after stretching, and l0 is the initial length. Its optical response is investigated when subjected to stress by applying uniaxial stretching along the X and Y axes. When the stretch is along the X axis, the positive and negative CD bands undergo a redshift as the strain increases because stretching changes the geometry and optical path of the structure, which alters the resonance condition of the modes. This makes the resonant peaks move away from their original spectral positions. The magnitude of the negative CD band decreases, while the positive band remains nearly unchanged.

On the other hand, a substantially stronger spectral response is obtained when stretching is applied along the y axis. Redshifts are noticeable in both positive and negative CD bands, but the spectral displacement of the longer wavelength negative CD resonance is much greater than that of the X direction stretching. It can also be seen that the positive CD band has the same magnitude of CD, while the magnitude of the negative CD band decreases significantly. This indicates an anisotropic chiral response of the structure, as the dominant chiral modes are more aligned with the structural features along the y direction according to this behaviour. The variation of Q factor corresponding to mode 1 and 2 when the structure is subjected to stretch is also shown in figure 6. With increasing stretch, the Q factor consistently decreases in the X direction for both modes whereas the Y direction shows a non-monotonic behaviour for both as the Q value initially decreases and then increases at higher stretch while in the second mode it fluctuates before declining.

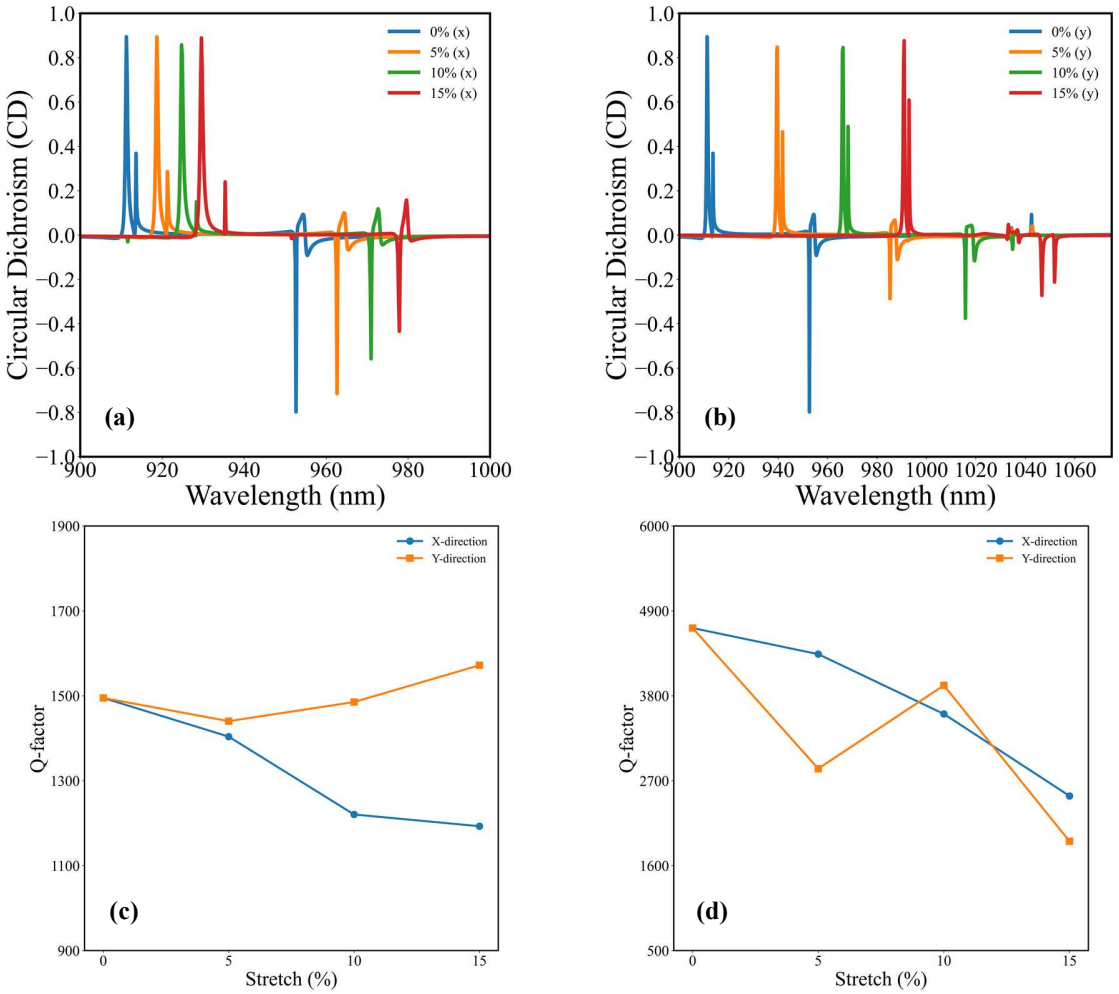

Figure 6. (a) Circular dichroism vs wavelength for stretching along x axis. (b) Circular dichroism vs wavelength for stretching along y axis. (c) and (d) show variation of Q factor of modes 1 and 2 with stretch along x and y direction respectively.

CHAPTER 4

CONCLUSION AND FUTURE PERSPECTIVE

This chapter concludes the main results of the proposed work, states the original scientific contributions, reflects critically on the limitations of the study, discusses the practical implications of the results, and identifies the most promising directions for future research. Together, these constitute a comprehensive assessment of what has been achieved and what remains to be explored.

A dual band CD response has been demonstrated using a single layer PDMS based chiral metasurface under oblique incidence. By breaking both in plane and out of plane symmetry, introduced by the orientation of the cavities, strong chiroptical responses are produced which lead to distinct chiral resonant modes. The magnitude of CD is very high, about 0.89 at 911 nm which implies that at this wavelength, LCP is suppressed and -0.8 at 952 nm which implies that RCP is suppressed. This preferential transmission can be confirmed with the electric field distribution. The metasurface provides high Q factors of ~1495 and ~4678 at resonance frequency. Parametric studies show that a small change in the geometry of the structure still gives high CD values with some spectral shifts and a possible change in the behaviour of mode 2. Furthermore, the flexible nature of PDMS allows continuous and anisotropic modulation of the CD response under uniaxial stretching, with minimum decline of resonance behaviour. These results show that a simple and efficient platform can be designed to achieve mechanical tunability with polarization selective metasurfaces with potential applications in sensing, tunable filtering, and compact chiral photonic systems.

There are limitations to this work that should be addressed. The works is entirely numerical based so there are no experimental fabrication or optical measurements performed to support the

results. The accuracy depends on the correctness of the material model given by Zhang et al. [30]. Real PDMS samples may vary in refractive index depending on curing conditions, ageing, and humidity absorption, which could possibly shift the resonant wavelengths relative to the simulated values. The mechanical model has been simplified using geometric scaling without accounting for the full three-dimensional Poisson contraction. The study also considers uniaxial stretching which is not encountered in wearable device scenarios where biaxial and shear deformation takes place.

REFERENCES

[1] E. Basar, M. Di Renzo, J. de Rosny, M. Debbah, M. S. Alouini, and R. Zhang, "Wireless Communications Through Reconfigurable Intelligent Surfaces," ArXiv, 2019, doi: 10.48550/arXiv.1906.09490.

[2] T. Cui, M. Qi, X. Wan, J. Zhao, and Q. Cheng, "Coding metamaterials, digital metamaterials and programmable metamaterials," Light: Science & Applications, vol. 3, p. e218, 2014, doi: 10.1038/lsa.2014.99.

[3] V. Sharma, Y. Kalra, and R. K. Sinha, "Modelling and design of human eye inspired concentric cylindrical metalens," Optical Communications, vol. 565, Aug. 2024, doi: 10.1016/j.optcom.2024.130627.

[4] L. Ai, Z. Gan, C. Vannahme, and X. Zhu, "Application of metasurface in future displays," Nanophotonics, pp. 3527–3555, 2025, doi: 10.1515/nanoph 2025 0269.

[5] C. M. Soukoulis and M. Wegener, "Past achievements and future challenges in the development of three dimensional photonic metamaterials," Nature Photonics, vol. 5, pp. 523–530, 2011, doi: 10.1038/nphoton.2011.154.

[6] N. I. Zheludev, "The Road Ahead for Metamaterials," Science, vol. 328, pp. 582–583, 2010, doi: 10.1126/science.1186756.

[7] Z. Xing, J. Liao, Z. Xu, X. Cheng, and J. Zhang, "The Design of Highly Reflective All Dielectric Metasurfaces Based on Diamond Resonators," Photonics, vol. 11, p. 1015, 2024, doi: 10.3390/photonics11111015.

[8] A. I. Kuznetsov et al., "Optically resonant dielectric nanostructures," Science, vol. 354, p. aag2472, 2016, doi: 10.1126/science.aag2472.

[9] C. U. Hail, A. K. U. Michel, D. Poulikakos, and H. Eghlidi, "Optical Metasurfaces: Evolving from Passive to Adaptive," Advanced Optical Materials, vol. 7, p. 1801786, 2019, doi: 10.1002/adom.201801786.

[10] L. Kang, R. P. Jenkins, and D. H. Werner, "Recent Progress in Active Optical Metasurfaces," Advanced Optical Materials, vol. 7, p. 1801813, 2019, doi: 10.1002/adom.201801813.

[11] M. V. Gorkunov, A. A. Antonov, V. R. Tuz, A. S. Kupriianov, and Y. S. Kivshar, "Bound States in the Continuum Underpin Near Lossless Maximum Chirality in Dielectric Metasurfaces," Advanced Optical Materials, vol. 9, p. 2100797, 2021, doi: 10.1002/adom.202100797.

[12] E. Petronijevic, A. Belardini, G. Leahu, R. Li Voti, and C. Sibilia, "Nanostructured materials for circular dichroism and chirality at the nanoscale," Optical Materials Express, vol. 12, p. 2724, 2022, doi: 10.1364/OME.456496.

[13] X. Kong, L. V. Besteiro, Z. Wang, and A. O. Govorov, "Plasmonic Chirality and Circular Dichroism in Bioassembled and Nonbiological Systems," Advanced Materials, vol. 32, 2018, doi: 10.1002/adma.201801790.

[14] A. Zhu, W. Chen, A. Zaidi et al., "Giant intrinsic chiro optical activity in planar dielectric nanostructures," Light: Science & Applications, vol. 7, p. 17158, 2018, doi: 10.1038/lsa.2017.158.

[15] V. Sharma, Y. Kalra, and R. K. Sinha, "Chiral perovskite based metasurface for linear and circular dichroism," Journal of Optics, vol. 26, p. 125103, 2024, doi: 10.1088/2040 8986/ad80a7.

[16] Z. Hu, Y. Sun, H. Dong, H. Fan, K. Ding, Y. Jin et al., "Recent Advances in Dielectric Chiral Metasurfaces," Advanced Physics Research, vol. 4, no. 6, 2025, doi: 10.1002/apxr.202400187.

[17] Q. M. Deng, X. Li, M. X. Hu, F. J. Li, X. Li, and Z. L. Deng, "Advances on broadband and resonant chiral metasurfaces," npj Nanophotonics, vol. 1, no. 1, 2024, doi: 10.1038/s44310 024 00018 5.

[18] P. Tonkaev, I. Toftul, Z. Lu, H. Qin, S. Qiu, W. Yang et al., "Nonlinear Chiral Metasurfaces Based on Structured van der Waals Materials," Nano Letters, vol. 24, no. 34, pp. 10577–10582, 2024, doi: 10.1021/acs.nanolett.4c02765.

[19] T. Badloe, J. Lee, J. Seong, and J. Rho, "Tunable Metasurfaces: The Path to Fully Active Nanophotonics," Advanced Photonics Research, vol. 2, p. 2000205, 2021, doi: 10.1002/adpr.202000205.

[20] T. Fadhil and A. Al Sahlawi, "Recent Developments in Active Metamaterials and their Practical Applications," Al Iraqia Journal for Scientific Engineering Research, vol. 4, pp. 47–54, 2025, doi: 10.58564/IJSER.4.2.2025.317.

[21] R. Kowerdziej, A. Ferraro, D. C. Zografopoulos, and R. Caputo, "Soft Matter Based Hybrid and Active Metamaterials," Advanced Optical Materials, vol. 10, no. 19, 2022, doi: 10.1002/adom.202200750.

[22] J. Qin, S. Jiang, S. Li, S. He, and W. Zhu, "Microfluidic Metasurfaces: A New Frontier in Electromagnetic Wave Engineering," Advanced Physics Research, vol. 3, no. 11, 2024, doi: 10.1002/apxr.202400059.

[23] J. Li, J. Chen, D. Yan, F. Fan, K. Chen, K. Zhong et al., "A Review: Active Tunable Terahertz Metamaterials," Advanced Photonics Research, vol. 5, no. 7, 2024, doi: 10.1002/adpr.202300351.

[24] X. He, W. Cao, and F. Lin, "Tunable BIC metamaterials with Dirac semimetals," Nanophotonics, vol. 14, no. 27, pp. 4875–4925, 2025, doi: 10.1515/nanoph 2025 0358.

[25] K. Fan, R. D. Averitt, and W. J. Padilla, "Active and tunable nanophotonic metamaterials," Nanophotonics, vol. 11, no. 17, pp. 3769–3803, 2022, doi: 10.1515/nanoph 2022 0188.

[26] D. Han, L. Zhang, M. Becton, and X. Chen, "Mechanical Deformation Induced Circular Dichroism in Propeller Shaped Terahertz Metamaterials," Advanced Materials Technologies, vol. 6, no. 6, 2021, doi: 10.1002/admt.202100161.

[27] X. Li, H. Jiang, J. Lin, W. Zhu, and W. Zhao, "Large range strength switchable circular dichroism in a mechanically reconfigurable chiral metasurface," Optical Communications, vol. 563, p. 130615, 2024, doi: 10.1016/j.optcom.2024.130615.

[28] Z. Liu, Y. Xu, C. Ji, S. Chen, X. Li, X. Zhang et al., "Fano Enhanced Circular Dichroism in Deformable Stereo Metasurfaces," Advanced Materials, vol. 32, no. 8, 2020, doi: 10.1002/adma.201907077.

[29] X. Guan, S. Xie, J. Zhuo, and S. Sun, "Tunable circular dichroism supported by quasi bound states in the continuum of a stretchable metasurface," Physica B: Condensed Matter, vol. 699, p. 416867, 2025, doi: 10.1016/j.physb.2024.416867.

[30] X. Zhang, J. Qiu, X. Li, J. Zhao, and L. Liu, "Complex refractive indices measurements of polymers in visible and near infrared bands," Applied Optics, vol. 59, pp. 2337–2344, 2020.

[31] E. Plum, V. A. Fedotov, and N. I. Zheludev, "Specular optical activity of achiral metasurfaces," Applied Physics Letters, vol. 108, p. 141905, 2016.

[32] C. Menzel, C. Rockstuhl, and F. Lederer, "Advanced Jones calculus for the classification of periodic metamaterials," Physical Review A, vol. 82, 2010.

[33] A. G. Ardakani and K. Moradi, "Strong circular dichroism in a non chiral metasurface based on an array of metallic V shaped nanostructures," European Physical Journal Plus, vol. 133, p. 73, 2018, doi: 10.1140/epjp/i2018 11909 0.

[34] R. Xu, J. Luo, J. Sha, J. Zhong, Z. Xu, Y. Tong et al., "Stretchable IR metamaterial with ultra narrowband perfect absorption," Applied Physics Letters, vol. 113, p. 101907, 2018, doi: 10.1063/1.5044225.